A gain-of-function screen for genes controlling motor axon guidance and synaptogenesis in *Drosophila*

Rachel Kraut*, Kaushiki Menon* and Kai Zinn

Background: The neuromuscular system of the *Drosophila* larva contains a small number of identified motor neurons that make genetically defined synaptic connections with muscle fibers. We drove high-level expression of genes in these motor neurons by crossing 2293 GAL4-driven EP element lines with known insertion site sequences to lines containing a pan-neuronal GAL4 source and UAS-green fluorescent protein elements. This allowed visualization of every synapse in the neuromuscular system in live larvae.

Results: We identified 114 EPs that generate axon guidance and/or synaptogenesis phenotypes in F1 EP x driver larvae. Analysis of genomic regions adjacent to these EPs defined 76 genes that exhibit neuromuscular gain-of-function phenotypes. Forty-one of these (known genes) have published mutant alleles; the other 35 (new genes) have not yet been characterized genetically. To assess the roles of the known genes, we surveyed published data on their phenotypes and expression patterns. We also examined loss-of-function mutants ourselves, identifying new guidance and synaptogenesis phenotypes for eight genes. At least three quarters of the known genes are important for nervous system development and/or function in wild-type flies.

Conclusions: Known genes, new genes, and a set of previously analyzed genes with phenotypes in the *Adh* region display similar patterns of homology to sequences in other species and have equivalent EST representations. We infer from these results that most new genes will also have nervous system loss-of-function phenotypes. The proteins encoded by the 76 identified genes include GTPase regulators, vesicle trafficking proteins, kinases, and RNA binding proteins.

Address: Division of Biology, California Institute of Technology, Pasadena, California 91125, USA.

Correspondence: Kai Zinn
E-mail: zinnk@its.caltech.edu

*R.K. and K.M. contributed equally to this work.

Received: **11 January 2001**
Revised: **8 February 2001**
Accepted: **8 February 2001**

Published: **20 March 2001**

Current Biology 2001, 11:417–430

0960-9822/01/$ – see front matter

Background

The neuromuscular system of the *Drosophila melanogaster* larva provides one of the best experimental frameworks in which to identify and study genes that control axon guidance, synaptogenesis, and regulation of synaptic strength. The muscle innervation pattern is relatively simple and highly stereotyped, with only 32 motor neurons and 30 muscle fibers per abdominal hemisegment [1] (reviewed by [2]). The growth cones of these motor neurons reach their muscle targets during late embryogenesis, and then differentiate into an almost invariant pattern of type I neuromuscular junction (NMJ) synapses.

In this paper, we describe a P element–based gain-of-function (GOF) screen for gene products that cause alterations in the larval neuromuscular system when they are expressed at high levels in motor neurons. Such GOF screens allow identification of genes that participate in neural development but also have roles in earlier developmental processes. The GOF strategy also sensitizes the screen and minimizes the problem of genetic redundancy. This is because pan-neuronal overexpression of transcriptional regulators, neural cell surface proteins, and signaling molecules can produce strong effects on motor axon guidance and/or synaptogenesis, even when loss-of-function (LOF) mutations in the same genes produce only weak phenotypes that would be missed in a screen [3–8, 9]. Overexpression/misexpression screens are inherently risky, however, in that high-level expression of a gene in a particular cell type may produce phenotypes even when the gene in question is not normally involved in the development of that cell type.

We used the EP modular misexpression system devised by P. Rorth, which employs a P-transposable element containing 14 copies of the UAS element that responds to the yeast transcription factor GAL4, linked to a basal promoter sequence [10, 11]. In a cell that expresses GAL4, a transcript that initiates within the EP element and propagates into adjacent DNA will be produced. If an EP is inserted in the appropriate orientation 5′ to a gene (most P element insertion sites are close to transcription start

sites), one can direct high-level transcription of that gene in a particular cell type by crossing the EP line to a driver line [12] in which GAL4 is expressed in that cell type.

We screened a set of 2293 EP lines with known insertion site sequences [10, 13]. EP-driven expression from these lines can be effectively used for gene identification, because the UAS element functions as part of a promoter but does not work as an enhancer [10, 11]. Only the first coding region within a eukaryotic mRNA will normally be translated, and transcriptional terminators separate most genes. Thus, if an EP drives overexpression of the gene closest to the 3′ end of the element, one can generally assume that this EP will not affect expression of genes further away. Since our screen is done on F1 animals bearing only one copy of the EP, one can also assume that most EPs will not produce LOF phenotypes.

Each EP line was crossed to a driver line containing a pan-neuronal GAL4 source and a UAS-green fluorescent protein (GFP) construct. In the F1 progeny from such crosses, transcription from the EP is driven in neurons, and these neurons also contain large amounts of GFP. Because the GFP readily enters axons and presynaptic terminals, one can visualize individual boutons in each NMJ through the translucent cuticle of live larvae.

We identified 114 EP insertions that produced strong F1 phenotypes when crossed to the driver line. We examined the genome sequence [14] flanking each of these EPs, and selected a subset for further study in which the EP is adjacent to a transcription unit that exhibits homology to other sequences in the database. This analysis identifies 41 "known genes," which we define here as those for which mutations have already been described in published papers. We assembled published phenotypic and expression data on these genes, and examined larval neuromuscular LOF phenotypes for some of them ourselves. These results show that at least three quarters of the known genes identified by the GOF screen are important for nervous system development or function in wild-type flies.

We then describe 35 "new genes" that are of particular interest because of the proteins they encode and/or because they have strong or unique GOF phenotypes. New genes are defined here as those without published mutations. An analysis of homology relationships displayed by the known gene and new gene sets, using criteria established by Ashburner and colleagues [15], suggests that most of the new genes will also have neural LOF phenotypes. The products that are encoded by the genes identified in our screen include kinases, protein and lipid phosphatases, Rho family GTPases, guanine nucleotide exchange factors (GEFs), GTPase-activating proteins (GAPs), ATPases, cell surface receptors, RNA binding proteins, transcriptional regulators, and a variety of other proteins likely to be involved in protein trafficking, modification, and degradation.

Results

Visualization of motor axons and synapses in live larvae using GFP

To drive the expression of EP-linked genes in motor neurons, we used the X-linked C155 (*elav*) element [5], which expresses GAL4 in all postmitotic neurons. This was combined with autosomal UAS-GFP elements to make driver lines, collectively denoted as C155;GFP, which simultaneously confer expression of the EP-linked gene and of GFP when crossed to EP insertion lines (see Materials and methods in Supplementary material published with this article on the Internet). The complete pattern of type I NMJ synapses can be visualized in live third instar larvae from C155;GFP lines (Figure 1b–c contains photographs through the larval cuticle).

Figure 1a is a composite confocal microscope image of the five main motor nerve branches in a larval abdominal hemisegment. These are: the main ISN branch, which travels furthest and innervates dorsal muscles, passing two intermediate branchpoints on its way; SNa, which bifurcates and innervates lateral muscles; ISNb (also known as SNb), which innervates ventrolateral muscles (VLMs); and ISNd (also known as SNd) and SNc, which innervate separate groups of ventral muscles (reviewed in [2]).

In our screen, we primarily scored the five main branch trunks, the presence of the ISN second branchpoint and the SNa bifurcation, and the presence and morphology of the following synapses: ISN on dorsal muscles 1, 2, 3 (internal layer), 9, and 10 (external layer); ISNb on muscles 12, 13, 6/7, 14, and 30, SNa on muscles 5, 8, and 21–24, and ISNd on muscles 15, 16, and 17 (see Figure 1a).

At this larval stage, the synapses and muscles they innervate are in distinct layers, and these can be clearly visualized in C155;GFP larvae by double staining with anti-GFP antibody and phalloidin. Figure 2 shows pseudo-three-dimensional volume-rendered views of the internal and external muscle layers of a larva, displaying axons and ISNb/ISNd synapses. The complex morphologies of individual synapses are clearly observable with the GFP marker.

Execution of the screen

To conduct the screen, we crossed males from second and third chromosome EP lines to C155;GFP driver line females, and females of X chromosome lines to C155;GFP males. The resultant fluorescent F1 offspring then all contained one copy each of C155-GAL4, UAS-GFP, and the EP insertion. The axonal GFP signal was dimmer in

Figure 1

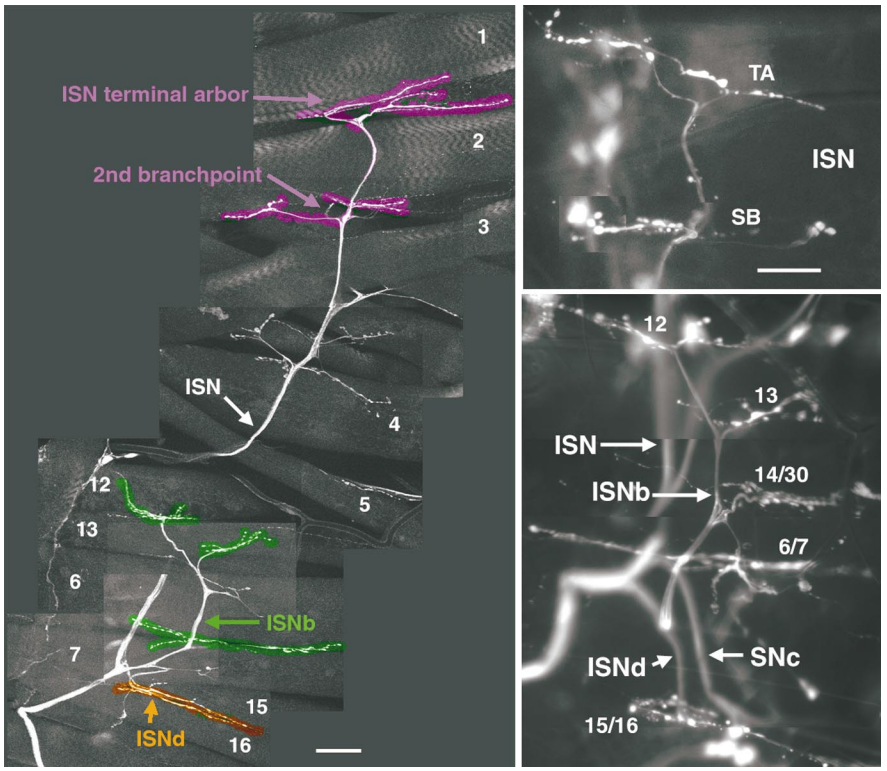

The pattern of neuromuscular synapses in wild-type third instar larvae. **(a)** A composite of several confocal *z*-series images of an abdominal hemisegment of a third instar C155;GFP larval fillet stained with anti-GFP antibody. The ISN, ISNb, and ISNd nerve trunks, the ISN terminal arbor and second branchpoint, and some muscle fibers are labeled. The apparent gap in the ISN is caused by the shift in focal planes between different *z*-series. SNa is not visible in this focal plane. Synapses scored in our screen are indicated by colored shading, including dorsal ISN synapses onto muscles 1 and 2, ISNb synapses onto muscles 6/7, 13, and 12, and ISNd synapses onto muscles 15/16. The scale bar represents 28 μm. **(b,c)** Synapses in live C155;GFP third instar larvae visualized by GFP fluorescence, photographed with a Magnafire digital camera through a 40× water immersion lens on a Zeiss Axioplan. (b) Shown are the terminal arbor (TA) and second branchpoint (SB) of the ISN. (c) Shown are ISNb and ISNd synapses. Synapses on muscles 12, 13, 6/7, 30/14, and 15/16 are labeled. Note that individual synaptic boutons are clearly visible. Dorsal is up and posterior is to the right in all panels in this paper. The scale bar for (b,c) represents 10 μm.

these F1s than in homozygous C155;GFP larvae, but could still be easily visualized in live animals (see Figures 4–5). Behavioral prescreens were conducted for some crosses (see Materials and methods).

Missing or abnormal synapses and pathfinding errors are very rare in C155;GFP (or F1 C155;GFP x wt) larvae. In our screen, we classified F1 EP x driver animals with two or more hemisegments with altered synapses, or which displayed connectivity errors in multiple hemisegments, as having an abnormal phenotype. EP lines producing phenotypes were recrossed for confirmation.

The observed phenotypes were difficult to separate into

Figure 2

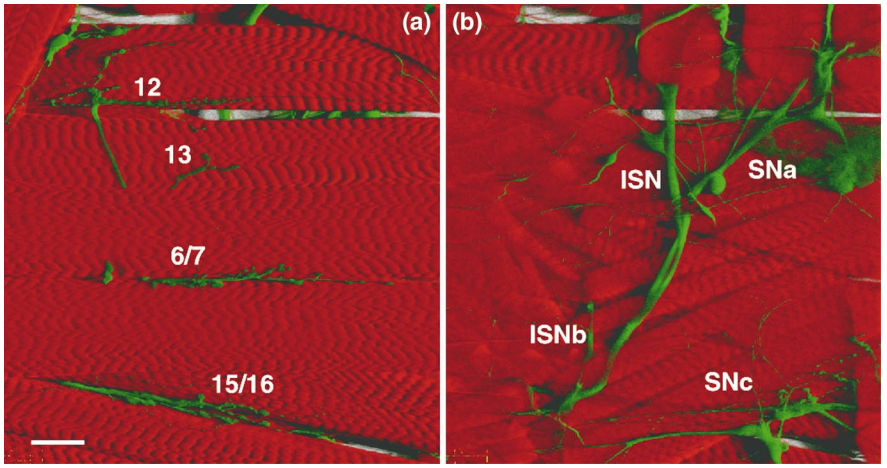

Volume-rendered views of wild-type motor axons, synapses, and muscles. Neurons in C155;GFP larvae were labeled with anti-GFP (green), and muscles are labeled with rhodamine-phalloidin (red). These images show the actual paths of the nerves through the three-dimensional muscle field. **(a)** View from the interior of the ISNb, ISNd, and the ventrolateral and ventral muscles (numbered). **(b)** View from the exterior. (This is a mirror image of what one would actually see if one examined the back of [a], so [a] and [b] can be directly superimposed). SNa and SNc are visible in this plane. Arrows in (b) indicate PNS neurons along the SNa and SNc nerves. The cloudy cell at the upper right of (b) is an unidentified cell type that also expresses GFP in this driver line. The scale bar represents 40 μm. The views were generated from confocal *z*-series images with the Imaris program (Bitplane AG, Switzerland).

Figure 3

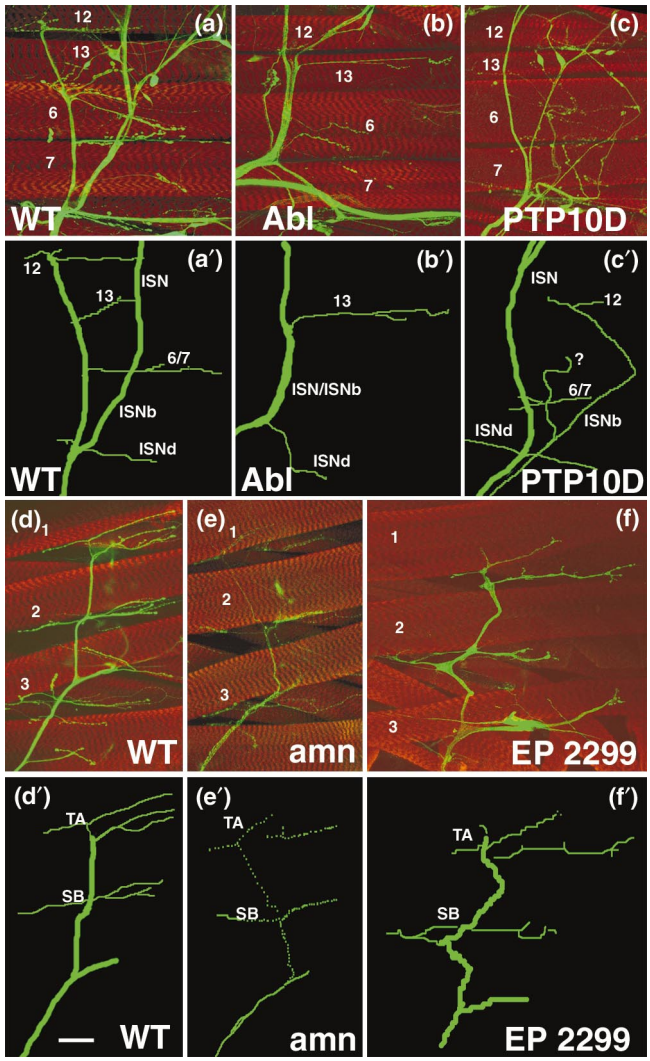

Confocal images of overexpression phenotypes observed in the screen. Third instar larval fillets were stained with anti-GFP (green) and rhodamine-phalloidin (red). **(a)** ISNb and ISNd in C155;GFP (wild-type), showing normal synapses onto muscles 12, 13, and 6/7. A tracing of the ISN, ISNb, and ISNd branches and synapses is shown in (a′). **(b,b′)** Pathfinding errors of entire nerve branches: an EP(3)3101 x C155;GFP F1 larva overexpressing the Abl tyrosine kinase displays an ISNb fusion bypass phenotype, in which ISNb fails to defasciculate from the ISN and muscle 13 is innervated by an abnormal side branch. **(c,c′)** Pathfinding errors by individual axons: an EP(X)1172 x C155;GFP F1 larva overexpressing the DPTP10D tyrosine phosphatase displays a strong phenotype in which ISNb axons separate from each other after leaving the ISN and wander over the surfaces of the muscle fibers. SNa, SNc, and the common nerve trunk to the next posterior segment are also visible in (a–c), but are not included in the tracings in (a′–c′). **(d,d′)** The distal ISN in C155;GFP, showing normal synapses onto muscles 1, 2, and 3 and more external muscles. TA indicates terminal arbor synapses; SB indicates second branchpoint synapses. **(e,e′)** Reduced synapses: an EP(X)0346 x C155;GFP F1 larva overexpressing the Amnesiac gene product displays a phenotype in which the distal ISN and its synaptic branches are very thin and synapses are reduced in size. This is not due to a reduction in GFP expression in these larvae, as proximal nerve trunks contain normal amounts of GFP. **(f,f′)** Altered ISN synapses in an EP(2)2299 x C155;GFP F1 larva overexpressing DBEACH1 mRNA. Note the abnormal bulges at the junctions between the axons and the synaptic branches. The scale bar represents 40 μm.

distinct groups, as they involve complex alterations in the targeting of nerve branches and the morphologies of synapses at both normal and abnormal sites. To generate a preliminary categorization, we assigned phenotypes to three broad classes: (A) Pathfinding. This class includes truncations and defasciculation failures of entire nerve branches, as well as missing branchpoints and individual axons with abnormal trajectories. (B) Morphologically altered, reduced, or missing synapses. This class includes synapses with abnormal branching geometries. Defects such as abnormally small boutons or boutons with distorted morphologies are also included. (C) Excess or ectopic synapses. This class includes synapses at the wrong sites and synapses that are much larger than normal. We recognize that the A, B, and C classes are likely to lump together phenotypes that arise from different kinds of cellular defects. Nevertheless, this scheme provided a straightforward way to create an initial grouping of the EP lines.

Abnormal larvae often exhibited multiple phenotypes that spanned even these broad categories. We thus classified the 114 EP lines that generated larvae with strong motor neuron connectivity defects when crossed to C155;GFP by listing all the phenotypic classes observed in F1 larvae (see Table S1 in Supplementary material). Most crosses displayed phenotypes in two or more classes, with class A being the most common (78%). Class B was also common (66%). Excess/ectopic synapses (class C) were observed for 30% of crosses. Note that some class B and C abnormal synapse phenotypes might be a consequence of earlier pathfinding errors. Forty-one of the 114 crosses displayed only one class of phenotype; of these, 21 had phenotype A, 16 had phenotype B, and 4 had phenotype C.

Analysis of GOF phenotypes

Figure 3 displays confocal images of dissected larvae stained with anti-GFP antibody, showing characteristic overexpression phenotypes for four genes identified in the screen: *Abl* (cytoplasmic tyrosine kinase gene), *Ptp10D* (receptor tyrosine phosphatase [RPTP] gene), *amnesiac* (neuropeptide gene), and a gene encoding a large protein related to human Chediak-Higashi syndrome protein (denoted here as DBEACH1; see Table S4). All four of these genes are expressed in the CNS of wild-type embryos (Figure S2; Table S5) [16–19].

Overexpression of *Abl* causes severe pathfinding defects (fusion bypass phenotypes) in which ISNb fails to defasciculate from the ISN (Figure 3b,b′). Similar bypass pheno-

types were previously observed in stage 16/17 embryos overexpressing *Abl* [8]. *Ptp10D* overexpression larvae have strong pathfinding phenotypes in which ISNb axons defasciculate from each other and wander around the VLM field, often failing to reach their muscle targets (Figure 3c,c′). The *Abl* and *Ptp10D* phenotypes, although clearly distinct, both fall within class A. *amnesiac* overexpression larvae have abnormally thin axons and synaptic branches, so that the distal section of the ISN in these larvae has a withered appearance (class B; Figure 3e,e′). Driving overexpression of DBEACH1 mRNA from EP2299 produces an interesting phenotype in which the distribution of cytoplasm between the axon and synapse is altered, so that bulges or knots form at synaptic branch junctions. The synaptic branching pattern is also abnormal (class B; Figure 3f,f′).

In Figures 4, 5, and S1, we show composite images of live F1 larvae from crosses of a C155;GFP driver to 15 different EP lines. Figure 4 displays characteristic ISNb and ISNd phenotypes for five EPs that confer class A (axonal pathfinding) phenotypes. These EPs drive the overexpression of *pins* (*Rapsynoid*), CG8487 (encodes a sec7 family GEF), CG1691 (encodes an mRNA localization protein), CG13349 (encodes a cell surface protein), and *center divider* (encodes a kinase; see Table S4 for evidence and annotations for EPs of Figures 4, 5, and S1). A variety of complex abnormal axonal branching patterns are observed, suggesting that ISNb and/or ISNd axons make incorrect pathfinding and outgrowth decisions at several different choice points when these genes are overexpressed. Abnormal synaptic geometries and ectopic synapses (class B and C phenotypes) are also observed for some of these EPs.

Figure 5 shows characteristic class B and C (abnormal synapse) ISNb and ISN phenotypes for five EPs. Panneuronal expression of these EP-linked genes primarily affects terminal synaptic branches. *Fat facets* overexpression alters ISN terminal arbor geometry (d,d′), while *egalitarian* overexpression causes expansion of type II synapses (e,e′). The other EPs that are represented here drive the expression of *apontic*, CG18445 (encodes an O-acyltransferase related to Porcupine), and CG10426 (encodes a polyphosphoinositide 5-phosphatase).

Figure S1 displays additional complex phenotypes that are characterized by pathfinding errors, extra axonal branches, and ectopic synapses. The five EPs shown drive the expression of *pebble*, CG5643 (encodes a PP2A regulatory B subunit), CG6811 (encodes a p50-RhoGAP), and CGs 1210 and 7719 (these encode kinases).

Twelve of the EP lines that we identified in our screen (EPs 1335, 1508, 2299, 2289, 2306, 2587, 3415, 0381, 0815, 3208, 3474, and 3559) were found to produce visible adult external sensory (ES) organ (bristle) phenotypes when crossed to the *scabrous*-GAL4 driver [20]. A total of 105 lines generated phenotypes in the ES organ screen, so there is about an 11% overlap in the loci identified by the two screens. EPs 0609, 1353, and 3403 were also identified in a screen for modifiers of rough eye phenotypes produced by the overexpression of a dominant-negative KSR kinase mutant. A total of 13 EPs generated phenotypes in this screen [21]. EPs 0355 and 3101 were identified in the original EP screens described in [10]; only a few EPs were individually reported in this paper. EP2582 (drives *roundabout 2*) was identified by its GOF CNS phenotype in a screen for midline crossing defects [22].

Known genes identified in the screen: molecular characterization

Having defined EP lines that produced phenotypes when crossed to C155;GFP, we analyzed the genomic sequences [14] around these EP insertion sites in order to evaluate which genes were likely to be transcribed from the EP elements (see Materials and methods). Table S2 describes the relationships of the 114 EPs to known and predicted genes. Most EPs that produce phenotypes (>80%) are located in an orientation (denoted as +/+) that would generate GAL4-driven sense strand mRNAs for all or part of a nearby gene. This was also observed in the other two published screens of these EP lines [10, 20]. Some, however, are within genes in the opposite (−/+) orientation, and might generate neural LOF phenotypes by the production of antisense RNAs (see [10] for examples; also [23]). About 8% of the EPs are not located near any candidate gene.

Forty-three EP elements among the collection of 114 are within or adjacent to 41 known genes (Table S3). For 32 of these, the EP element is inserted 5′ to the entire coding region. The insertion sites are usually just upstream of the mRNA start, in the 5′ UTR, or in the first (noncoding) intron (see Table S4 for precise localization). These EPs probably produce phenotypes by driving high-level expression of the wild-type gene product. For six genes (*amnesiac*, *ash2*, *Neurexin*, *nuclear fallout*, *pumilio*, and *toutvelu*), the EP is in the +/+ orientation within the gene, so that the predicted EP-driven transcript would not encode the entire protein. The protein fragments whose expression is driven by these EPs may have wild-type function in some cases, and may act as dominant negatives in other cases (the predicted expressed fragments are analyzed in Tables S3 and S4). Finally, for the *scab* (*Volado*), *schnurri*, and *Uba1* genes, the EP is inserted within an intron in the −/+ orientation.

We examined the relationships of the proteins encoded by the known genes to other protein sequences in the databases, and found that 37/41 (90%) display significant

Figure 4

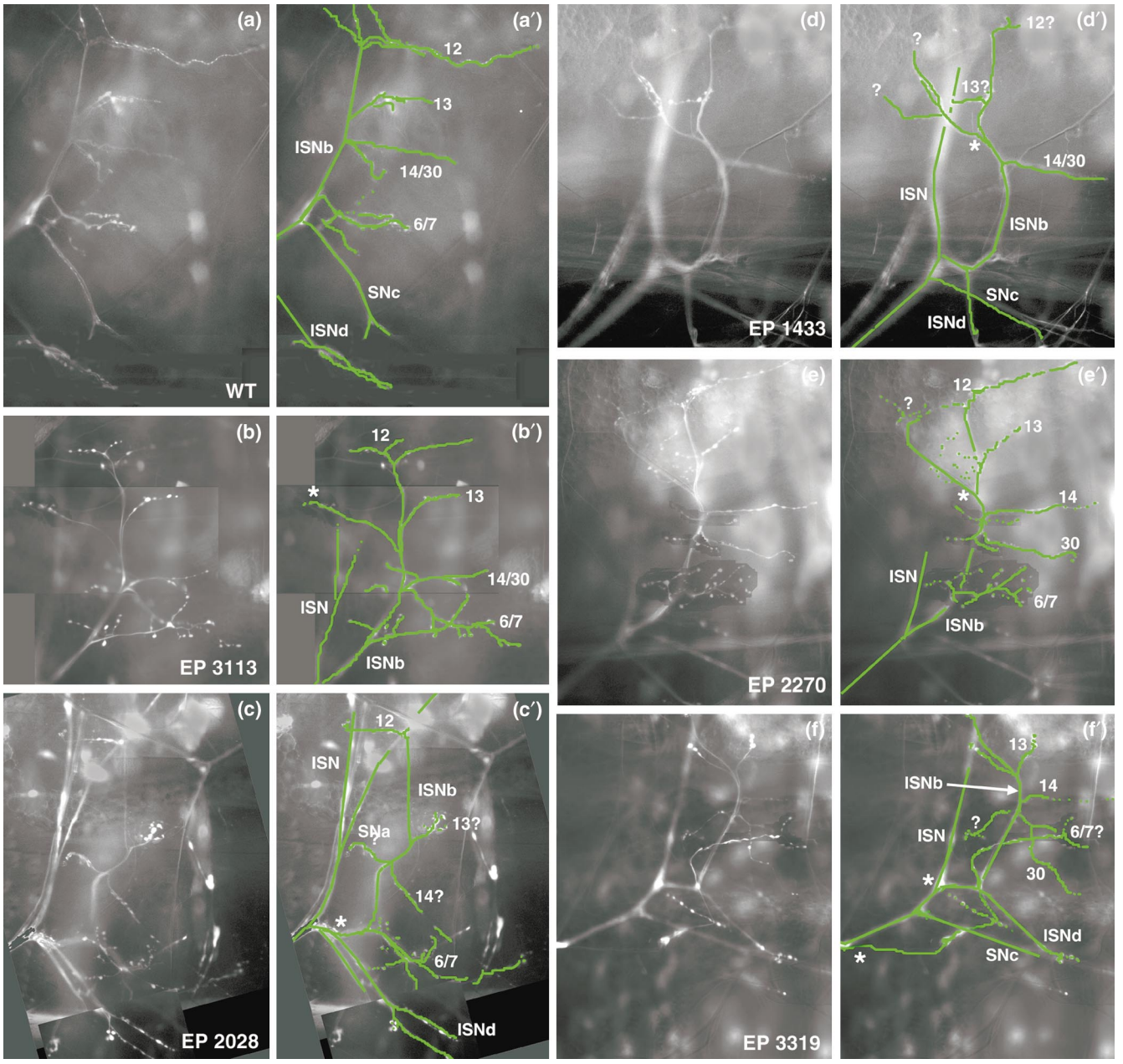

Pathfinding phenotypes in F1 EP x driver larvae. Composite Magnafire photographs of ventral muscle regions of live third instar larvae are shown, paired with tracings of some of the axonal pathways in these hemisegments. **(a,a′)** Wild type. ISNb synaptic branches on muscles 12, 13, 14, 30, and 6/7 are indicated, as are ISNd and the initial segment of SNc (out of focus in [a]). **(b,b′)** EP3113, overexpressing *pins*. An abnormal axonal/synaptic branch is observed (*), and the 6/7 synapse (normally linear, as in [a]) has a highly branched structure. **(c,c′)** EP2028, overexpressing CG8487 (encodes a sec7-GEF). The entire structure of the ISNb is abnormal. **(d,d′)** EP1433, overexpressing CG1691 (encodes an mRNA localization protein). ISNb leaves the ISN at an abnormal point. It generates an abnormal axonal branch (*) that splits into synaptic branches (?) on incorrect muscles. (We provisionally denote branches as axonal or synaptic based on whether they have boutons [white bead-like structures].) **(e,e′)** EP2270, overexpressing CG13349 (encodes a cell surface protein). An abnormal axonal branch (*) and many extra synaptic branches are observed. **(f,f′)** EP3319, overexpressing *center divider*. An unidentified branch (lower *) leaves the ISN and travels up into the region normally innervated by ISNb; this branch may form synapses on 6/7. Other abnormal branches from ISNb are also observed (?).

homology to proteins in other (noninsect) species. 25/41 (61%) are related to proteins in other (noninsect) species with alignment scores (E values) of better (less) than e-50, and 19/41 (46%) with scores of better than e-100 (Table S3). Thirty-nine of the 41 genes have *Drosophila* EST matches.

Figure 5

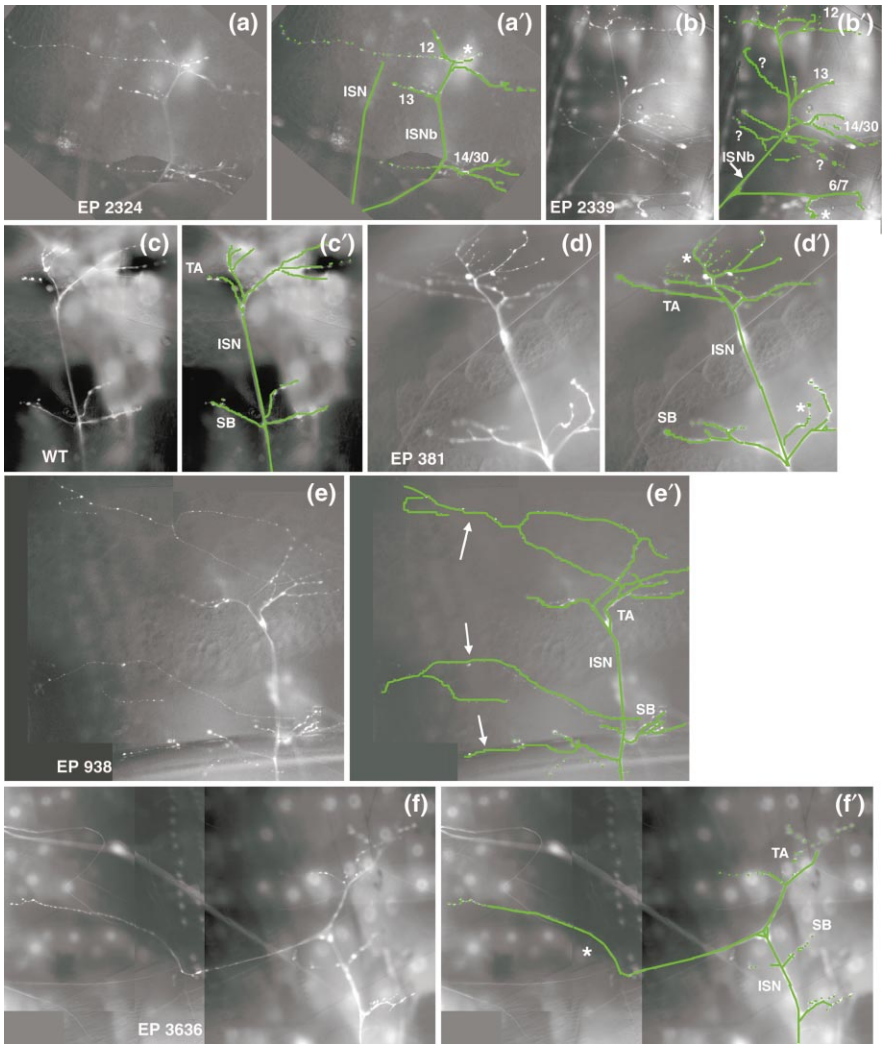

Synaptic phenotypes in F1 EP x driver larvae. **(a,a′)** EP2324, overexpressing CG18445 (encodes an O-acyltransferase). The structure of the muscle 12 synapse is abnormal (*). **(b,b′)** EP2339, overexpressing *apontic*. The 6/7 synapse is abnormal, having a small branch with a large distorted bouton-like shape (*); many incorrect synaptic branches are also observed (?). The remainder of the panels shows dorsal muscle regions. **(c,c′)** Wild-type ISN. The terminal arbor (TA) and second branchpoint (SB) are labeled. **(d,d′)** EP0381, overexpressing *fat facets*. The synapses at SB and TA have abnormal structures, with a spray of extra branches (*) emanating from the terminal arbor. **(e,e′)** EP0938, overexpressing *egalitarian*. Type II synaptic branches, which innervate all muscles but do not have a highly stereotyped morphology, extend from the ISN and cover a much larger than normal area (arrows), as if their outgrowth has been facilitated. **(f,f′)** EP3636, overexpressing CG10426 (encodes a polyphosphoinositide 5-phosphatase). A long abnormal branch (*) with bouton-like structures emanates from the ISN and crosses the segmental border.

This distribution of homology scores for the genes identified in our screen is remarkably similar to that found in a detailed analysis of the 49 known genes with detectable phenotypes that can be assigned to open reading frames (ORFs) within the 2.9 Mb *Adh* region, which has been subjected to saturation mutagenesis. 90% of these genes have noninsect relatives, 63% have scores of better than e-50 versus these relatives, and 37% have scores of better than e-100 [15]. Almost all of the genes have EST matches.

Known genes identified in the screen: phenotypic analysis

One cannot usually draw strong conclusions about the normal functions of genes from an analysis of their GOF phenotypes. The major value of a GOF screen resides in its ability to rapidly identify genes for further study. In this paper, therefore, our primary aim is to use this collection of known genes to estimate the fraction of all genes identified through neuromuscular GOF phenotypes that are likely to be important for nervous system development or function in wild-type flies. The first criterion for such genes is that they should be expressed in the nervous system in wild-type embryos. At least 33 of the 41 genes are normally expressed in the CNS (Table S3; Figure S2). Such expression, however, is a necessary rather than a sufficient criterion, given that CNS expression is displayed by a large fraction of genes: >50% of *Adh*-region known genes (10/19 analyzed thus far) and 24% (227/927) of the genes represented by the CK EST collection are expressed in the CNS [24]; (see [15]). Motor neuron cell bodies are not identifiable in most in situ hybridization photographs, so expression data usually cannot prove that neuromuscular GOF phenotypes are due to overexpression rather than to misexpression.

The second, and more important, aspect of the analysis of known genes is to determine what fraction of these genes has nervous system LOF phenotypes. We found that most (28 of 41) have already been described in pub-

Figure 6

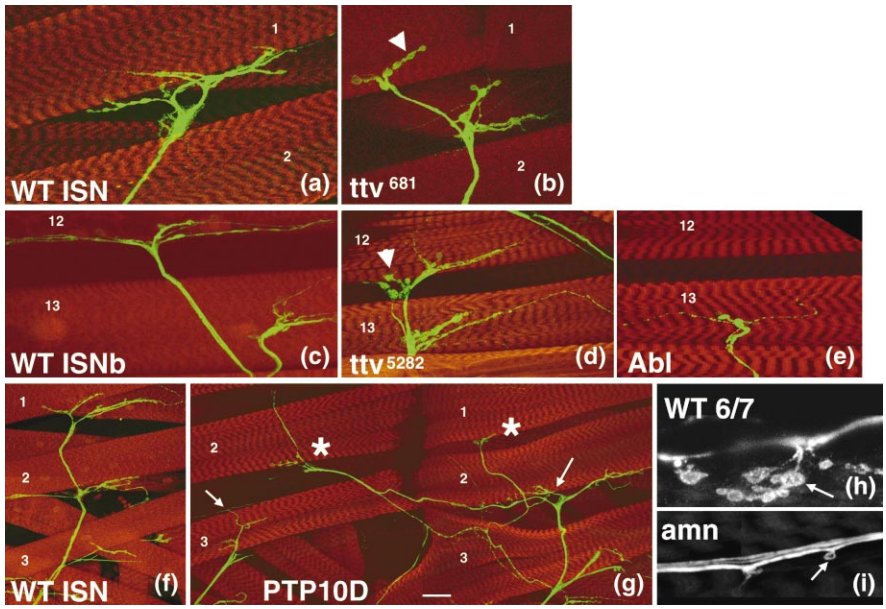

Loss-of-function phenotypes of known genes. Confocal images of fillets of wild-type and mutant third instar larvae stained with a mixture of mAbs 1D4 and 22C10 to visualize axons and synapses (green), and with rhodamine-phalloidin to visualize muscles (red). **(a)** Wild-type ISN terminal arbor synapses onto muscle 1. **(b)** Abnormally large boutons (arrowhead) in a *tout-velu*^{681} larva. **(c)** Wild-type ISNb synapses onto muscles 12 and 13. **(d)** A *tout-velu*^{5282} larva also has abnormally large ISNb boutons (arrowhead). **(e)** An *Abl*^{1}/*Abl*^{4} mutant larva in which ISNb fails to innervate muscle 12. **(f)** Wild-type ISN synapses onto muscles 1, 2, and 3 and more external muscles. **(g)** Two hemisegments of a *Ptp10D*^{1} mutant larva, showing truncated ISNs (arrows) that fail to innervate dorsal muscles. Collateral branches extend from the ISN in the right hemisegment, forming ectopic synapses (asterisks) onto dorsal muscles in both hemisegments. (h) Boutons (one indicated by an arrow) in the wild-type synapse on muscles 6/7. (i) A 6/7 synapse in an *amn*^{EP710} larva has a greatly reduced number of boutons. Only one small bouton is visible in this panel (arrow). The scale bar for (a–e) represents 14 μm; for (f,g), 40 μm; for (h,i), 6 μm.

lished work as having LOF phenotypes that affect the nervous system in some manner.

Sixteen genes (*Abl*, α-*adaptin*, *Adf1* [*nalyot*], *brakeless*, *Fasciclin 2*, *Gliotactin*, *Laminin A*, *mastermind*, *Neurexin*, *pebble*, *misshapen*, *Ptp10D*, *pumilio*, *purity-of-essence* [*pushover*], *roundabout 2*, and *spitz*) have published LOF phenotypes affecting axons and/or synapses. These phenotypes were examined using light-level antibody staining, ultrastructural analysis, and/or electrophysiology. For *mastermind*, *spitz*, and perhaps others, axonal defects may be secondary consequences of alterations in neuronal and/or glial cell fates.

amnesiac, *Volado*, and *nalyot* are learning/memory mutations. *bang senseless*, *easily shocked*, *pushover*, and *scribbler* (*brakeless*) mutations affect other aspects of behavior. Finally, *downstream of receptor kinase* (*drk*), *eIF-4A*, *fat facets*, *orbit*, *pins* (*Rapsynoid*), and *schnurri* affect neuronal cell fates (references for known gene phenotypes are cited in Table S3).

We obtained LOF mutants for many of these genes, and found third instar neuromuscular phenotypes for *Abl*, *amnesiac*, *egalitarian*, *Ptp10D*, *pumilio*, *pushover*, *tout-velu*, and *wunen*. *Abl* (tyrosine kinase) mutants lack the branch of ISNb that innervates muscle 12 (Figure 6e), and this muscle is sometimes innervated by an abnormal side branch from the ISN. This phenotype is derived from the *Abl* LOF phenotype previously described in stage 17 embryos, in which ISNb stalls at muscle 13 and the muscle 12 branch is absent [9]. *Ptp10D* null LOF mutants [25] have pathfinding defects such as ISN truncations and abnormal ISN and ISNb branching (Figure 6g). The penetrance of the truncated ISN phenotype in *Ptp10D*^{1} larvae is 31% (n = 66).

amnesiac LOF mutants have a phenotype in which very few boutons form at type I NMJs (Figure 6i). Less than 10% of the normal number of boutons are visible at muscle 6/7 synapses in *amnesiac* homozygotes (>30 synapses examined). *tout-velu* LOF mutants have abnormal synaptic morphologies, characterized by boutons that are too large (Figures 6b,d). Tout-velu is a heparan sulfate copolymerase related to human EXT tumor suppressors that is required for Hedgehog transport [26, 27].

pumilio larvae displayed pathfinding errors, and we found synaptic defects in *wunen*, *egalitarian*, and *pushover* mutants (Table S4). In summary, adding our data to the previously published results indicates that at least 31 of the 41 known genes (76%) have nervous system LOF phenotypes, and therefore are likely to be important for nervous system development and/or function in wild-type *Drosophila*. At least 19 genes have LOF phenotypes affecting axons and/or synapses.

We also evaluated whether our known gene set was en-

riched for genes with nervous system LOF phenotypes relative to the reference set of 49 *Adh*-region known genes [15]. (*Gliotactin* and *Ance* are members of both sets.) Six of these 49 (*beaten path*, *Ca-α1D*, *Gliotactin*, *kuzbanian*, *shuttle craft*, and *Son of sevenless* [*Sos*]) have published LOF phenotypes affecting axons and/or synapses. *Smi35A* mutations affect behavior, and *Suppressor of Hairless* (*Su[H]*) mutations alter PNS cell fates and affect mechanoreceptor physiology (references in [15]). These data indicate that our GOF screen selects for genes that have nervous system LOF phenotypes, since 28/41 (69%) from our screen have published neural phenotypes versus 8/49 (16%) for the *Adh*-region genes. Thus, while one can identify genes that are likely to have some detectable LOF phenotype simply by selecting those that are highly conserved [15], performing a GOF screen for phenotypes affecting a process of interest can produce a several-fold enrichment for genes that are specifically involved in that process.

It is interesting to compare the GOF and LOF phenotypes shown for *Abl*, *Ptp10D*, and *amnesiac* in Figures 3 and 6. For all three, the GOF phenotypes are much more easily visualized at low magnification than the LOF phenotypes, indicating that they would be easier to detect in a screen. The LOF and GOF phenotypes are not obviously opposite in sign, however, so one could not predict the nature of the LOF phenotypes from an examination of the GOF phenotypes.

Characterization of new genes identified by GOF phenotypes

After examining genomic regions around the 72 EP insertions that are not adjacent to known genes, we identified those that are near predicted genes (CGs) and/or cDNAs with homology to other sequences in the database. We selected 37 EPs for further analysis that are in the +/+ orientation to 34 new genes that are of subjective interest to us, either because of the products they encode or because they produce strong or unique GOF phenotypes. One −/+ EP, 3607, was also selected (see Table S4 for insertion site localization data).

Like the known genes described above, the new genes have a homology score distribution that is very similar to that of the 49 known genes in the *Adh* region [15]. 33/35 (94%) of the predicted proteins encoded by the new genes have noninsect relatives, 22/35 (63%; versus 60% for our known genes and 63% for *Adh*-region genes) have scores of better than e-50 against these relatives, and 11/35 (31%; versus 45% for our known genes and 37% for *Adh*-region genes) have scores of better than e-100. 34/35 of the new genes have at least one *Drosophila* EST match.

The analysis of homology scores and EST representations addresses the concern that, because they had not previously been genetically characterized, the new genes we identified might resemble the 145 genes in the *Adh* region that are predicted to lack LOF phenotypes, rather than the 49 genes that do have such phenotypes. The "no phenotype" *Adh* set, however, behaves very differently from our new gene and known gene sets: 54% have relatives in other noninsect species, but only 14% have scores versus these relatives that are better than e-50, and 2% have scores better than e-100. Of those genes with relatives, only 26% are represented by ESTs [15].

Note that the selection of our new gene set was partially based on homology relationships with other genes, most of which were in noninsect species, so the percentage of these genes that has noninsect relatives is not meaningful. Numerical score values and EST matches were not part of the selection process, however, so the fact that the new genes are highly conserved and have ESTs argues that they will behave phenotypically like the known gene set. Thus, we expect that most of the new genes will also have nervous system LOF phenotypes.

We have examined the wild-type expression patterns of 18 of the 35 new genes by in situ hybridization, and two others were examined previously. These patterns are all described in Table S5. Figure S2 shows whole-mount wild-type embryos that are hybridized to probes for 17 different genes. We also show a representative EP x driver F1 embryo, displaying overexpression of CG11172 mRNA. All 18 of the new genes we examined are overexpressed in EP x driver F1 embryos (Table S5).

Our results show that 13 of these 20 new genes are expressed in the CNS at higher levels than in other tissues. Of these, however, only CG1691 (mRNA localization protein) mRNA is expressed exclusively in the CNS in wild-type late embryos. Four other genes are ubiquitously expressed, or are expressed in the CNS at lower levels than in other tissues. Three genes are not expressed in the CNS at detectable levels. In summary, our data are consistent with, but do not prove, the hypothesis that the GOF phenotypes of 17 of the 20 new genes examined thus far are due to overexpression rather than to misexpression.

In Tables 1 and S4, we have assembled new genes and known genes together into seven categories, based on the proteins they encode. These are: (1) GTPases, GEFs, GAPs, and putative GTP/ATP binding proteins (9 members, 1 known gene); (2) protein kinases, protein phosphatases, and lipid phosphatases (13 members, 5 known genes); (3) a diverse collection of proteins likely to be involved in protein degradation, protein trafficking, and localization within cells, and/or in covalent modification of proteins, lipids, or carbohydrates (15 members, 6 known genes); (4) putative signaling proteins that contain defined protein–protein interaction or Ca^{2+} binding domains, and which are not members of the other groups (5 members,

Table 1

Known genes and new genes identified in our screen (see Table S4 for annotations, functional information, and references).

Gene	EP	Molecular information
GTPases/GEFs/GAPs/GTP binding proteins		
CG9366, RhoL	EP(3) 0888	A member of Rac/Rho/Cdc42 family of small GTPases.
pebble, CG8114	EP(3) 3415	Known gene; Rho-GEF involved in actin reorganization.
CG 8487, sec7 family GEF	EP(2) 2028	Sec7-related GEFs act on ARF GTPases.
CG3862, RCC GEF-related protein	EP(2) 1242	Some RCC proteins are GEFs for Ran family nuclear GTPases.
CG18640 (Bj1), RCC protein (−/+)	EP(3) 3630	RCC protein, the apparent ortholog of vertebrate RCC.
CG 6811, p50Rho-GAP	EP(3) 3152	A GTPase-activating protein for Rho family GTPases.
CG5521, related to tuberin Rap-GAPs	EP(3) 0527	Rap1 is a small GTPase that antagonizes Ras.
CG 2017, GP-1 related	EP(3) 3503	Ortholog of GTPBP2, a mammalian GTP binding protein.
CG11411, 8D8.1	EP(X) 1336	Large protein with an ATP/GTP binding motif.
Kinases and phosphatases		
Abl, CG4032	EP(3) 3101	Known gene; tyrosine kinase.
Ptp10D, CG1817	EP(X) 1172	Known gene; receptor tyrosine phosphatase on motor neurons.
center divider, CG6027	EP(3) 3319	Known gene; S/T kinase orthologous to human TESK.
misshapen, no CG	EP(3) 0549, 0609	Known gene; Ste20-like S/T kinase.
CG7719-related, S/T kinase	EP(3) 0515	Related to fly Wts/Lats tumor suppressor kinase.
CG1210 (Pk61C), S/T kinase	EP(3) 3553	3-phosphoinositide-dependent protein kinase.
CG17090, S/T kinase	EP(3) 3571	Ortholog of mammalian homeodomain-interacting kinases.
CG6297, JIL-1 S/T kinase	EP(3) 3657	Tandem S/T kinase associated with chromosomes.
CG7001, Bin4 S/T kinase	EP(X) 0438	A member of S6 kinase family.
CG5643, PP2A B subunit	EP(3) 3559	Ortholog of B56 family of PP2A phosphatase regulatory B subunits.
wunen, CG8804	EP(2) 2208	Known gene; transmembrane phosphatidate phosphatase (PAP).
CG8805, Wunen2/Tunen	EP(2) 2607	Also a PAP; gene adjacent to *wunen*.
CG10426, pharbin-like	EP(3) 3636	An inositol polyphosphate 5-phosphatase.
Protein degradation/trafficking/modification		
fat facets, CG1945	EP(3) 0381	Known gene; ubiquitin C-terminal hydrolase.
Uba 1, CG1782 (−/+)	EP(2) 2609	Known gene; E1 ubiquitin-activating enzyme.
lemming, CG18042	EP(2) 2077	Known gene; related to E3 ubiquitin–protein ligases.
CG1341 (Rpt1), AAA ATPase	EP(2) 2153	Ortholog of vertebrate AAA ATPase MSS1.
α-adaptin, CG4260	EP(2) 0896	Known gene; clathrin adaptor subunit.
CG 8487, sec7 family GEF	EP(2) 2028	see notes above
CG10426, pharbin-like	EP(3) 3636	see notes above
CG8604, Amphiphysin	EP(2) 2443	Ortholog of amphiphysin, a regulator of endocytosis.
CG17762, Tomosyn	EP(X) 1359, 1562	Ortholog of synaptic vesicle protein tomosyn.
CG9011/14001, DBEACH1	EP(2) 2299	Related to human Chediak-Higashi syndrome/mouse Beige proteins.
pins (Rapsynoid), CG5692	EP(3) 3113	Known gene; TPR repeat protein that complexes with Inscuteable.
CG3249, PKA anchor protein	EP(X) 1400	Related to vertebrate KH domain PKA anchor proteins.
tout-velu, CG10117	EP(2) 0765	Known gene; heparan sulfate copolymerase related to human EXTs
CG18445, O-acyltransferase	EP(2) 2324	A multispan transmembrane protein related to fly Porcupine.
Putative signaling proteins with protein–protein interaction and/or Ca_{2+} binding domains		
drk, CG6033	EP(2) 2477	Known gene; SH2-SH3 adapter.
pushover, CG14472	EP(2) 0737	Known gene; huge Ca^{2+}/CaM binding protein.
CG1435, CBP Ca^{2+} binding protein	EP(X) 1201	Member of a family of EF hand CBPs found only in invertebrates.
CG 6017, ankyrin domain	EP(3) 3292	Related to Hyph huntingtin binding protein.
CG10977, MSP protein	EP(3) 3539	Related to mammalian VAMP/synaptobrevin-associated (VAP) protein.

(*continued*)

2 known genes); (5) known or putative transcriptional regulators (12 members, 9 known genes); (6) RNA binding proteins, putative helicases, and enzymes that act on RNA (10 members, 5 known genes); (7) putative plasma membrane or secreted proteins (15 members, 10 known genes). Many genes are listed twice, given that they have attributes that fit more than one category. This classification provides a framework in which to think about how the proteins might function in axon guidance and synaptogenesis.

Discussion

In this paper, we describe an overexpression/misexpression screen to identify genes that are involved in axon guidance and synaptogenesis in the *Drosophila* larval neuromuscular system. To perform the screen, we crossed a

Table 1

Continued

Gene	EP	Molecular information
Putative transcriptional regulators		
bang senseless, CG12223	EP(X) 0355	Known gene; HMG box transcriptional repressor.
crooked legs (), CG14938	EP(2) 2226	Known gene; Zn finger proteins.
Kr-h1, CG9167	EP(2) 2289	Known gene; Zn finger protein.
Adf 1 (nalyot), CG15845	EP(X) 0815	Known gene; transcription factor.
mastermind, CG8118	EP(2) 2575	Known gene; Q-rich nuclear protein of unknown function.
ash2, CG6677	EP(3) 3472	Known gene; trithorax-like transcriptional activator.
HLHm7, CG8361	EP(3) 3587	Known gene; E(spl) complex HLH protein.
schnurri, CG7734 (−/+)	EP(2) 0644	Known gene; Zn finger transcription factor.
scribbler (brakeless), CG5580	EP(2) 2461	Known gene; nuclear protein required for R cell axon targeting.
CG11172, Rel domain protein	EP(X) 1335, 1353, 1508	Related to mammalian nuclear factor of activated T cells (NFAT).
CG4427, Sp1-like Zn finger protein	EP(2) 2237	Closest fly relative is Sp1, CG1343.
CG17090, S/T kinase	EP(3) 3571	see notes above
RNA binding proteins and helicases		
egalitarian, CG4051	EP(2) 0938	Known gene; related to Werner syndrome helicase.
eIF-4A, CG9075	EP(2) 1011	Known gene; DEAD box helicase, translation initiation factor.
eIF-4E, CG4035	EP(3) 0568	Known gene; mRNA cap binding protein.
pumilio, CG9755	EP(3) 3038	Known gene; RNA binding protein and translational regulator.
apontic, CG5393	EP(2) 2339	Known gene; binds to Oskar mRNA together with Bruno.
CG16788, RRM domain protein	EP(3) 1082	Related to vertebrate splicing factors, but no clear orthologs.
CG1691, KH domain protein	EP(X) 1433	Ortholog of vertebrate beta-actin mRNA zipcode binding protein.
CG3613, qkr58E-1, KH domain	EP(2) 2103	In an 8-gene family of fly KH domain RNA binding proteins.
CG3249, PKA anchor protein	EP(X) 1400	see notes above
CG11486, polyA-nuclease related	EP(3) 3109	Ortholog of yeast Pan3p, a subunit of the polyA-nuclease.
Putative plasma membrane/secreted proteins		
amnesiac, CG11937	EP(X) 0346, 1571	Known gene; thought to encode a neuropeptide.
Fasciclin 2, CG3665	EP(X) 1462	Known gene; Ig-CAM related to vertebrate N-CAM.
***roundabout 2*, no CG**	EP(2) 2582	Known gene; Ig/FN domain protein involved in repulsive signaling.
Gliotactin, CG3903	EP(2) 2306	Known gene; esterase-related glial cell surface protein.
Laminin A, CG10236	EP(3) 3678	Known gene; the only fly laminin A chain.
Neurexin, CG6827	EP(3) 0809	Known gene; transmembrane protein at septate junctions.
Ptp10D, CG1817	EP(X) 1172	see notes above
scab (Volado), CG8095 (−/+)	EP(2) 2591	Known gene; α-integrin subunit.
spitz, CG10334	EP(2) 2632	Known gene; EGF-related transmembrane protein.
CG1762, Integrin βν	EP(2) 2235	An integrin β subunit exclusively expressed in the gut.
CG7607/CG14141?, Ig domain	EP(3) 3548	Two Ig domain CGs may be linked to form this gene.
wunen, CG8804	EP(2) 2208	see notes above
CG8805, Wunen2/Tunen	EP(2) 2607	see notes above
CG13101, related to Rolling Stone	EP(2) 2247	A member of a 6-gene multispan transmembrane protein family.
CG13349, membrane glycoprotein	EP(2) 2270	Related to mouse adhesion regulating molecule.

Known genes are listed by name in italics, followed by a descriptor and a CG number. New genes are listed by CG number, followed by a descriptor. The genes are grouped into categories described in the text.

set of 2293 lines containing insertions of the EP element, which contains a GAL4-driven enhancer/promoter [10, 11] to driver lines expressing GAL4 in all postmitotic neurons. The driver lines also contain UAS-GFP elements that allow visualization of individual boutons in every type I NMJ of live (Figure 1) or dissected (Figure 2) third instar larvae. One hundred and fourteen EP insertions that produced axon pathfinding or synaptic phenotypes were identified (Table S1; Figures 3–5, S1). Because the insertion site sequences of all of the EPs are known [13], we could identify the genes whose expression they are likely to affect. The GOF phenotypes do not define the normal function of these genes during neural development. Their primary value is in providing a method for rapid identification of genes for further study.

We found EP elements adjacent to 41 known genes (those with published mutant alleles) in configurations indicating that they should affect expression of only these genes. To evaluate the functions of the known genes in the nervous system, we compiled published data on their phenotypes and expression patterns (Table S3). We also directly examined the neuromuscular systems of LOF mutant larvae, identifying previously undescribed path-

finding and synaptogenesis phenotypes for eight genes (Figure 6; Table S4). Our results indicate that more than three quarters of the known genes identified by the GOF screen are important for nervous system development or function in wild-type *Drosophila* (Table S3).

The GOF screen also identified 35 new genes that encode a variety of interesting proteins (Tables 1, S4). In order to evaluate whether similar fractions of the new gene and known gene sets are likely to have neural LOF phenotypes, we examined their homology relationships with sequences in other species. A study of genes within the *Adh* region has shown that those genes that are closely related to sequences in other (noninsect) species usually have LOF phenotypes, while "pioneer genes," or genes with relatives only in *Drosophila* typically do not. Highly conserved genes are also much more likely to have EST matches [15].

The homology score (E value) distributions and EST representations of the known gene and new gene sets identified in our screen are like those of the set of 49 genes in the *Adh* region that have LOF phenotypes. By contrast, the E value distributions and EST representations of the set of 145 genes in the *Adh* region that are predicted to lack phenotypes are very different from those of the gene sets described here (see Results; Tables S3, S4). This suggests that the known genes and new genes differ only in whether they have already been studied using genetics, and that similar fractions of the two gene sets are likely to have nervous system LOF phenotypes. Most new genes are expressed in the CNS in wild-type embryos (Table S5; Figure S2).

Table S4 presents a detailed analysis of the relationships of each of the new genes to other sequences in the database. (Table 1 is a list of the genes described in Table S4.) This is useful because it influences one's hypotheses about the possible origins of GOF phenotypes, and can guide the course of future experiments. It is usually impractical to study every member of a large gene set such as the one described here by the generation and analysis of LOF mutations, so careful choices of genes must be made. Similar problems are likely to be encountered by *Drosophila* workers who are using microarray expression analysis and other genomic strategies to identify collections of new genes potentially involved in the processes they wish to study.

If a gene has several close *Drosophila* relatives, the fact that it displays an overexpression/misexpression phenotype may suggest only that one of these related genes is important for the process in question. The relevant gene is not necessarily the one actually identified by the screen. Conversely, if a gene is unique in *Drosophila*, its identification in a GOF screen is more likely to indicate that the gene itself is relevant (see Table S4 annotations).

Possible functional groupings of the identified genes

It is premature to formulate specific hypotheses about the developmental roles of the new genes we have identified, given that we have not yet characterized their LOF phenotypes. In addition, the observation that a protein exhibits certain homologies does not necessarily define the cellular processes in which it participates. Nevertheless, there are some interesting patterns that emerge from considering the nature of the proteins encoded by the set of 76 genes for which we observe neuromuscular GOF phenotypes. Below, we briefly describe two potential linkages among these proteins. The annotations in Table S4 include additional patterns, defining overlapping collections of proteins that may be involved in cytoskeletal rearrangements, vesicle trafficking, regulation of cell adhesion, phosphoinositide metabolism and signaling, protein degradation, RNA localization, and transcriptional control.

Learning and memory mutants: *amnesiac*, *nalyot*, and *Volado*, three of the known genes we identified, have learning and memory phenotypes [28–30]. *amnesiac* mutants also have altered tolerance to ethanol [31]. All three of these genes are widely expressed in the CNS in wild-type animals [19, 29, 30].

amnesiac was predicted to encode a neuropeptide related to pituitary adenylyl cyclase–activating peptide (PACAP) [28, 31]. Our experiments showed that *amnesiac* LOF mutants have an NMJ phenotype in which few boutons form (Figure 4). This phenotype could be due to a reduction of cAMP levels in the motor neuron if the putative Amnesiac peptide acts, like PACAP, to increase adenylyl cyclase activity. Interestingly, neuronal overexpression of *dunce* (cAMP phosphodiesterase), which would also be predicted to reduce neuronal cAMP levels, produces a bouton loss phenotype that is similar to, although less severe than, the *amnesiac* LOF phenotype [32].

nalyot is a hypomorphic mutation affecting the expression of the Adf1 transcription factor. *nalyot* mutants display a 15% decrease in NMJ bouton numbers, and slight overexpression of Adf1 produces 12% increases [30]. We found that high-level neuronal overexpression of Adf1 generated strong pathfinding and synaptic phenotypes (Table S4). Adf1 is likely to have multiple functions, given that it was also identified in the ES organ GOF screen [20].

The *Volado* mutation affects the expression of an alternatively spliced mRNA encoding one of the Scab (αPS3) integrin isoforms [29]. We found that driving transcription from an EP insertion that would be predicted to generate

an antisense transcript affecting only the Volado-αPS3 mRNA generates anatomical NMJ phenotypes.

Amnesiac, Adf1, and αPS3 may be components of systems that regulate structural aspects of plasticity in both brain and NMJ synapses. Fasciclin 2, which was also identified in our screen, is another important regulator of synaptic structure in larvae [33]. Studies in both vertebrate and invertebrate systems show that structural plasticity is quite sensitive to changes in the levels of regulatory proteins, so neuronal overexpression of other synaptic regulators might also produce alterations in larval NMJs. This suggests that EP screens for neuromuscular phenotypes may provide a way to rapidly identify new proteins that are involved in regulation of plasticity in the adult brain. It will thus be of interest to test adult-viable hypomorphic or null mutations in some of the new genes we identified for learning and memory phenotypes.

Clathrin-mediated endocytosis: This mechanism is used for synaptic vesicle recycling in nerve terminals. Signaling through a variety of cell surface receptors also requires clathrin-mediated endocytosis. The AP2 adaptor proteins and clathrin are recruited to the plasma membrane, after which the vesicle invaginates, separates from the membrane, uncoats, and moves along the actin cytoskeleton into the cytoplasm, where it is routed to the appropriate destination (reviewed in [34]).

We found α-*adaptin*, which encodes the large subunit of the AP2 complex [35], among the known genes, and amphiphysin (CG8604) [36] and a polyphosphoinositide 5-phosphatase (PPI 5-Ptase, CG10426) among the new genes. The Fat Facets protein, also identified in our screen, is thought to deubiquitinate and stabilize the fly epsin ortholog, Liquid Facets [37]. Amphiphysin, epsin, and the PPI 5-Ptase synaptojanin are all required for endocytosis in yeast, *Caenorhabditis elegans*, and/or mammalian brain synapses (reviewed in [34]).

These proteins exist in macromolecular complexes: amphiphysin binds to clathrin, AP2, synaptojanin, and dynamin, while epsin binds to AP2 and clathrin (reviewed by [34, 38]). The PPI 5-Ptase we identified does not have obvious amphiphysin binding (proline-rich) motifs, but has a carboxy-terminal membrane-targeting sequence (see Table S4).

We do not know how the overexpression of the four proteins identified in our screen would affect endocytosis. An excess of α-adaptin, amphiphysin, or epsin might disrupt the assembly of protein complexes, while excess PPI 5-Ptase activity could increase the rate of vesicle uncoating [39] or affect other steps in the endocytosis process [40]. Overexpression of PPI 5-Ptases can also produce cytoskeletal changes [41, 42]. Our results do indicate, however, that it would be fruitful to examine LOF and GOF mutations affecting other components of the clathrin-mediated endocytosis mechanism for nervous system phenotypes.

Supplementary material
Additional methodological details, tables, and figures are available with the electronic version of this article at http://www.current-biology.com/supmat/supmatin.htm.

Conclusions

In this study, we showed that an anatomical EP GOF screen of live larvae allows rapid molecular identification of a large number of genes that are potentially involved in axon guidance and synaptogenesis. We demonstrated that most of the known genes identified by our GOF screen are important for normal nervous system development and/or function. We also showed that an analysis of gene sets using only molecular information can have predictive value for genetic experiments, indicating whether genes identified in a screen are likely to display LOF phenotypes. Finally, organization of the identified gene sets into categories based on their sequence relationships may provide insights into the cell biology of neuromuscular development.

Acknowledgements

We thank Violana Nesterova for excellent technical assistance; Cyrus Papan for creating the volume-rendered views of Figure 2; Erik Griffin for screening some of the X chromosome lines; Haig Keshishian for instruction in larval dissection and staining methods; Haig Keshishian and Barry Dickson for the UAS-GFP line; Marc Halfon for the UAS-2×-EGFP line; Todd Laverty (UC Berkeley) and Tom Kidd and Jason Melendez (Exelixis) for EP lines; Steve Crews, Inge The, Ken Howard, James DeZazzo, and the Bloomington Stock Center for mutant lines; Guochun Liao, Nomi Harris, and Sima Misra (BDGP) for information about EP flanking sequences and general assistance with databases; the BDGP, Flybase, and Celera Genomics, without whom this work would not have been possible; and Aloisia Schmid, Benno Schindelholz, Nina Sherwood, and Anna Salazar (Zinn group) for helpful discussions and comments on the manuscript. See http://www.caltech.edu/~zinn/ for further information on motor axons. R.K. was supported by an NRSA postdoctoral fellowship from the NIH. This work was supported by NIH grant NS28182 to K.Z.

References

1. Schmid A, Chiba A, Doe CQ: **Clonal analysis of *Drosophila* embryonic neuroblasts: neural cell types, axon projections, and muscle targets.** *Development* 1999, **126:**4653-4689.
2. Keshishian H, Broadie K, Chiba A, Bate M: **The *Drosophila* neuromuscular junction: a model for studying development and function.** *Annu Rev Neurosci* 1996, **19:**545-575.
3. Thor S, Andersson SGE, Tomlinson A, Thomas JB: **A LIM-homeodomain combinatorial code for motor-neuron pathway selection.** *Nature* 1999, **397:**76-80.
4. Certel SJ, Clyne PJ, Carlson JR, Johnson WA: **Regulation of central neuron synaptic targeting by the *Drosophila* POU protein, Acj6.** *Development* 2000, **127:**2395-2405.
5. Lin DM, Goodman CS: **Ectopic and increased expression of Fasciclin II alters motoneuron growth cone guidance.** *Neuron* 1994, **13:**507-523.
6. Lin DM, Fetter RD, Kopczyinski C, Grenningloh G, Goodman CS: **Genetic analysis of fasciclin II in *Drosophila*: defasciculation, refasciculation, and altered fasciculation.** *Neuron* 1994, **13:**1055-1069.
7. Torroja L, Packard M, Gorczyca M, White K, Budnik V: **The *Drosophila* beta-amyloid precursor protein homolog promotes synapse differentiation at the neuromuscular junction.** *J Neurosci* 1999, **19:**7793-7803.
8. Wills Z, Bateman J, Korey CA, Comer A, Van Vactor D: **The tyrosine kinase Abl and its substrate Enabled collaborate with the receptor phosphatase Dlar to control motor axon guidance.** *Neuron* 1999, **22:**301-312.
9. Wills Z, Marr L, Zinn K, Goodman CS, Van Vactor D: **Profilin and the Abl tyrosine kinase are required for motor axon outgrowth in the *Drosophila* embryo.** *Neuron* 1999, **22:**291-299.

10. Rorth P, Szabo K, Bailey A, Laverty T, Rehm J, Rubin GM, *et al.*: **Systematic gain-of-function genetics in *Drosophila***. *Development* 1998, **125:**1049-1057.
11. Rorth P: **A modular misexpression screen in *Drosophila* detecting tissue-specific phenotypes.** *Proc Natl Acad Sci USA* 1996, **93:**12418-12422.
12. Brand AH, Perrimon N: **Targeted gene expression as a means of altering cell fates and generating dominant phenotypes.** *Development* 1993, **118:**401-414.
13. Liao GC, Rehm EJ, Rubin GM: **Insertion site preferences of the P transposable element in *Drosophila melanogaster*.** *Proc Natl Acad Sci USA* 2000, **97:**3347-3351.
14. Adams MD, Celniker SE, Holt RA, Evans CA, Gocayne JD, Amanatides PG, *et al.*: **The genome sequence of *Drosophila melanogaster***. *Science* 2000, **287:**2185-2195.
15. Ashburner M, Misra S, Roote J, Lewis SE, Blazej R, Davis T, *et al.*: **An exploration of the sequence of a 2.9-Mb region of the genome of *Drosophila melanogaster*: the Adh region.** *Genetics* 1999, **153:**179-219.
16. Henkemeyer MJ, West SR, Gertler FB, Hoffman FM: **A novel tyrosine kinase-independent function of *Drosophila abl* correlates with proper subcellular localization.** *Cell* 1990, **63:**949-960.
17. Tian S-S, Tsoulfas P, Zinn K: **Three receptor-linked protein-tyrosine phosphatases are selectively expressed on central nervous system axons in the *Drosophila* embryo.** *Cell* 1991, **67:**675-685.
18. Yang X, Seow KT, Bahri SM, Oon SH, Chia W: **Two *Drosophila* receptor-like tyrosine phosphatase genes are expressed in a subset of developing axons and pioneer neurons in the embryonic CNS.** *Cell* 1991, **67:**661-673.
19. DeZazzo J, Xia SZ, Christensen J, Velinzon K, Tully T: **Developmental expression of an amn(+) transgene rescues the mutant memory defect of amnesiac adults.** *J Neurosci* 1999, **19:**8740-8746.
20. Abdelilah-Seyfried S, Chan YM, Zeng CY, Justice NJ, Younger-Shepherd S, Sharp LE, *et al.*: **A gain-of-function screen for genes that affect the development of the *Drosophila* adult external sensory organ**. *Genetics* 2000, **155:**733-752.
21. Huang AM, Rubin GM: **A misexpression screen identifies genes that can modulate RAS1 pathway signaling in *Drosophila melanogaster*.** *Genetics* 2000, **156:**1219-1230.
22. Rajagopalan SEN, Vivancos V, Berger J, Dickson BJ: **Crossing the midline: roles and regulation of Robo receptors**. *Neuron* 2000, **28:**767-777.
23. Chen Y, Goodman RH, Smolik SM: **Cubitus interruptus requires *Drosophila* CREB-binding protein to activate wingless expression in the *Drosophila* embryo.** *Mol Cell Biol* 2000, **20:**1616-1625.
24. Kopczynski CC, Noordermeer JN, Serano TL, Chen WY, Pendleton JD, Lewis S, *et al.*: **A high throughput screen to identify secreted and transmembrane proteins involved in *Drosophila* embryogenesis**. *Proc Natl Acad Sci USA* 1998, **95:**9973-9978.
25. Sun Q, Bahri S, Schmid A, Chia W, Zinn K: **Receptor tyrosine phosphatases regulate axon guidance across the midline of the *Drosophila* embryo.** *Development* 2000, **127:**801-812.
26. The I, Bellaiche Y, Perrimon N: **Hedgehog movement is regulated through tout velu-dependent synthesis of a heparan sulfate proteoglycan.** *Mol Cell* 1999, **4:**633-639.
27. Toyoda H, Kinoshita-Toyoda A, Selleck SB: **Structural analysis of glycosaminoglycans in *Drosophila* and *Caenorhabditis elegans* and demonstration that tout-velu, a *Drosophila* gene related to EXT tumor suppressors, affects heparan sulfate in vivo.** *J Biol Chem* 2000, **275:**2269-2275.
28. Feany MB, Quinn WG: **A neuropeptide gene defined by the *Drosophila* memory mutant amnesiac.** *Science* 1995, **268:**869-873.
29. Grotewiel MS, Beck CDO, Wu KH, Zhu XR, Davis RL: **Integrin-mediated short-term memory in *Drosophila*.** *Nature* 1998, **391:**455-460.
30. DeZazzo J, Sandstrom D, de Belle S, Velinzon K, Smith P, Grady L, *et al.*: **nalyot, a mutation of the *Drosophila* Myb-related Adf1 transcription factor, disrupts synapse formation and olfactory memory.** *Neuron* 2000, **27:**145-158.
31. Moore MS, DeZazzo J, Luk AY, Tully T, Singh CM, Heberlein U: **Ethanol intoxication in *Drosophila*: genetic and pharmacological evidence for regulation by the cAMP signaling pathway.** *Cell* 1998, **93:**997-1007.
32. Cheung US, Shayan AJ, Boulianne GL, Atwood HL: ***Drosophila* larval neuromuscular junction's responses to reduction of cAMP in the nervous system.** *J Neurobiol* 1999, **40:**1-13.
33. Schuster CM, Davis GW, Fetter RD, Goodman CS: **Genetic dissection of structural and functional components of synaptic plasticity. I. Fasciclin-II controls synaptic stabilization and growth.** *Neuron* 1996, **17:**641-654.
34. Brodin L, Low P, Shupliakov O: **Sequential steps in clathrin-mediated synaptic vesicle endocytosis**. *Curr Opin Neurobiol* 2000, **10:**312-320.
35. GonzalezGaitan M, Jackle H: **Role of *Drosophila* alpha-adaptin in presynaptic vesicle recycling.** *Cell* 1997, **88:**767-776.
36. Razzaq A, Su Y, Mehren JE, Mizuguchi K, Jackson AP, Gay NJ, *et al.*: **Characterisation of the gene for *Drosophila* amphiphysin**. *Gene* 2000, **241:**167-174.
37. Cadavid AL, Ginzel A, Fischer JA: **The function of the *Drosophila* fat facets deubiquitinating enzyme in limiting photoreceptor cell number is intimately associated with endocytosis.** *Development* 2000, **127:**1727-1736.
38. Wigge P, McMahon HT: **The amphiphysin family of proteins and their role in endocytosis at the synapse.** *Trends Neurosci* 1998, **21:**339-344.
39. Cremona O, Di Paolo G, Wenk MR, Luthi A, Kim WT, Takei K, *et al.*: **Essential role of phosphoinositide metabolism in synaptic vesicle recycling**. *Cell* 1999, **99:**179-188.
40. Harris TW, Hartwieg E, Horvitz HR, Jorgensen EM: **Mutations in synaptojanin disrupt synaptic vesicle recycling**. *J Cell Biol* 2000, **150:**589-599.
41. Sakisaka T, Itoh T, Miura K, Takenawa T: **Phosphatidylinositol 4,5-bisphosphate phosphatase regulates the rearrangement of actin filaments.** *Mol Cell Biol* 1997, **17:**3841-3849.
42. Asano T, Mochizuki Y, Matsumoto K, Takenawa T, Endo T: **Pharbin, a novel inositol polyphosphate 5-phosphatase, induces dendritic appearances in fibroblasts**. *Biochem Biophys Res Commun* 1999, **261:**188-195.